Interpretation of Counterion Spin Relaxation in Polyelectrolyte Solutions

Bertil Halle,* Håkan Wennerström, and Lennart Piculell

Department of Physical Chemistry 1, University of Lund, Chemical Center, S-22007 Lund, Sweden
(Received: August 17, 1983)

A theory for quadrupolar spin relaxation of counterions in polyelectrolyte solutions is presented. The theory features a self-consistent mean-field cell description of the equilibrium distribution and the translational diffusion of the counterions. The residual electric field gradient (efg) is modeled as a short-ranged step-function perturbation. Complete randomization of the efg requires that a counterion diffuse from one polyion to another. This can be a very slow process, which then causes the efg correlation function to exhibit a (nearly exponential) long-time tail and the relaxation behavior to be dominated by the zero-frequency spectral density, $J(0)$. The central result of the theory is a simple expression for $J(0)$, with the residual efg as the only freely adjustable parameter. The theory accounts quantitatively for recent $^{23}Na^+$ transverse relaxation data from solutions of poly(acrylate) and poly(styrenesulfonate) as a function of polyion concentration, polyion charge density, and concentration of added salt. The resulting value (ca. 70 kHz) for the residual efg is consistent with results from quadrupolar line splittings. The invariance of the residual efg with respect to polyion dilution and protonation indicates that it is caused mainly by local short-range interactions. Under the experimental conditions considered, $J(0)$ appears to be unaffected by any changes in solution structure. In particular, it is not necessary to invoke a finite polyion persistence length or a finite orientational correlation between the polyions.

Introduction

The decisive factor that governs the behavior of polyelectrolyte solutions is the long-range Coulomb interaction which couples the polyions and the counterions.[1] As a consequence, the highly charged polyions tend to be distributed as far apart from each other as possible, while the counterions accumulate in the neighborhood of each polyion. These features are embodied in the commonly adopted cell model,[2,3] according to which the solution is divided into electroneutral cells of cylindrical symmetry, each containing a centrally located polyion along with its counterions and its share of any added salt. The counterion distribution within the cell is usually described within the Poisson–Boltzmann (PB) approximation, which, in the salt-free case, leads to an analytic solution.[4-6] The PB cell model approach has been used extensively to predict thermodynamic properties of polyelectrolyte solutions, usually resulting in excellent agreement with experimental data[3,7] and with computer simulations.[8]

While those equilibrium properties of polyelectrolyte solutions that depend mainly on the distribution of the counterions (and any added salt) are fairly well understood, much fundamental theoretical work remains to be done on the conformation and distribution of the polyions in polyelectrolyte solutions.[9] The major problem in constructing a general theory of the structure of polyelectrolyte solutions is the multitude of different length scales required to describe a macroscopically isotropic system composed of entities with one effectively infinite dimension and subject to long-range forces. One of these length scales, the electrostatic persistence length, has recently been treated at the PB level of approximation for an isolated polyion chain.[10,11] The structure of (salt-free) polyelectrolyte solutions at finite polyion concentration, however, remains a subject of considerable uncertainty and controversy.[12-15] It is only at very low polyion concentrations that one can confidently say something about the solution structure; if the concentration is so low that the cell diameter is much larger than the polyion contour length or its persistence length, then there should be no orientational correlation between polyions. At high concentrations (of order 10^{-1} monomolar) there exist small-angle X-ray[14,16] and neutron[15,17-19] scattering data that have been taken as indicative of a periodic ordering of the polyions. However, this interpretation may need revision.[69] In the present paper we shall be dealing with data obtained in the intermediate concentration range (10^{-4}–10^{-1} monomolar), which is essentially terra incognita as regards solution structure.

The technique of nuclear magnetic resonance (NMR) is potentially rich in information about equilibrium as well as dynamic properties of polyelectrolyte solutions. Under appropriately chosen experimental conditions, counterion nuclear spin relaxation can be used to study many facets of these intriguing systems, such as the distribution and translational diffusion of the counterions, intra- and interpolyion solution structure, and polyion dynamics. While this makes NMR an extremely powerful and versatile tool for studying polyelectrolyte solutions, it also calls for great care in the interpretation of experimental data.

We shall discuss two fundamentally different models for the interpretation of counterion spin relaxation: the site-exchange model and the mean-field model. (A similar interpretational dichotomy appears in connection with other transport properties, e.g., counterion self-diffusion.) According to the site-exchange model, a counterion can reside in either of a number of classes of equivalent discrete sites. The simplest, and most commonly adopted, version is the two-site-exchange model with a bound site, characterized by a stoichiometric association constant and a mean residence time (or a dissociation rate constant), and a free site with the properties of a dilute solution of a simple electrolyte. The

(1) F. Oosawa, "Polyelectrolytes", Marcel Dekker, New York, 1971.
(2) T. L. Hill, "Statistical Mechanics", Addison-Wesley, Reading, MA, 1960.
(3) A. Katchalsky, Z. Alexandrowicz, and O. Kedem in "Chemical Physics of Ionic Solutions", B. E. Conway and R. G. Barradas, Eds., Wiley, New York, 1966; A. Katchalsky, *Pure Appl. Chem.*, **26**, 327 (1971).
(4) R. M. Fuoss, A. Katchalsky, and S. Lifson, *Proc. Natl. Acad. Sci. U.S.A.*, **37**, 579 (1951).
(5) T. Alfrey, P. W. Berg, and H. Morawetz, *J. Polym. Sci.*, **7**, 543 (1951).
(6) S. Lifson and A. Katchalsky, *J. Polym. Sci.*, **13**, 43 (1954).
(7) E. Selegny, Ed., "Polyelectrolytes and Their Applications", Reidel, Dordrecht, 1975.
(8) D. Bratko and V. Vlachy, *Chem. Phys. Lett.*, **90**, 434 (1982).
(9) T. Odijk, *Lect. Notes Phys.*, **172**, 184 (1982).
(10) M. Le Bret, *J. Chem. Phys.*, **76**, 6243 (1982).
(11) M. Fixman, *J. Chem. Phys.*, **76**, 6346 (1982).
(12) P. G. de Gennes, P. Pincus, R. M. Velasco, and F. Brochard, *J. Phys. (Paris)*, **37**, 1461 (1976).
(13) T. Odijk, *Macromolecules*, **12**, 688 (1979).
(14) N. Ise and T. Okubo, *Acc. Chem. Res.*, **13**, 303 (1980).
(15) F. Nallet, J. P. Cotton, M. Nierlich, and G. Jannink, *Lect. Notes Phys.*, **172**, 175 (1982).
(16) N. Ise, T. Okubo, K. Yamamoto, H. Kawai, T. Hashimoto, M. Fujimura, and Y. Hiragi, *J. Am. Chem. Soc.*, **102**, 7901 (1980); N. Ise, T. Okubo, K. Yamamoto, H. Matsuoka, H. Kawai, T. Hashimoto, and M. Fujimura, *J. Chem. Phys.*, **78**, 541 (1983).
(17) M. Moan, *J. Appl. Crystallogr.*, **11**, 519 (1978).
(18) N. Nierlich, C. E. Williams, F. Boué, J. P. Cotton, M. Daoud, B. Farnoux, G. Jannink, C. Picot, M. Moan, C. Wolff, M. Rinaudo, and P. G. de Gennes, *J. Phys. (Paris)*, **40**, 701 (1979).
(19) F. Nallet, G. Jannink, J. B. Hayter, R. Oberthür, and C. Picot, *J. Phys. (Paris)*, **44**, 87 (1983)

0022-3654/84/2088-2482$01.50/0

site-exchange model is thus phrased in chemical terms and makes no explicit reference to the long-ranged forces involved. In particular, it treats all counterions residing in the free site as if they were dynamically equivalent. The counterion translational diffusion is thus replaced by a Markovian random walk in a discrete-state space. In the mean-field model, on the other hand, a counterion undergoes continuous translational diffusion in the mean field generated by the polyion and the counterions (and any added salt). The long-range Coulomb interaction is thus explicitly included in the model and no chemical association equilibrium is invoked. Instead, the polyion is characterized by its dimensions and charge distribution, usually modeled as a straight cylinder with a uniform surface charge density. In the dynamical description the polyion appears as a hard reflecting surface devoid of specific interactions. The counterion residence time at the polyion surface (as at any other point) is thus infinitesimal.

The site-exchange model has been used extensively to interpret NMR relaxation data from ions in solutions of charged macromolecules.[20-22] In many cases, the ion–macromolecule interaction is known to involve dehydration and direct coordination to specific liganding groups on the macromolecule. The site-exchange model should then provide an accurate description. (However, if the macromolecule carries a large net charge, the incorporation in the model of reencounter effects[23] may alter the interpretation of the deduced residence times.)

In the case of typical linear polyelectrolytes, such as poly(acrylate) (PAA) or poly(styrenesulfonate) (PSS), site binding (in the sense just described) does not seem to occur—at least not for monovalent counterions. Accordingly, counterion spin relaxation data from such systems have usually been interpreted in terms of a hybrid version of the site-exchange and mean-field models, which we shall call the state-exchange model. In the two-state-exchange model one retains the discrete-state description of the counterion dynamics, while the counterion distribution is regarded as being determined by the balance between long-range Coulombic and entropic forces (as, for example, in the PB approximation) rather than by the principle of mass action.[24] The bound state is then taken to comprise those counterions that reside within a certain distance from the polyion surface. This distance is usually chosen approximately as the diameter of a hydrated counterion, in accordance with the short range of the perturbation (characterized by the magnitude and the symmetry of the electric field gradient) that induces spin relaxation in quadrupolar counterion nuclei.[25] The observation, through line splittings in counterion NMR spectra, that the number of so-defined bound counterions is nearly invariant with respect to dilution, addition of salt, and changes in temperature provides unequivocal evidence in favor of a PB or ion condensation description (rather than a mass-action model) of the distribution of monovalent counterions in lyotropic liquid crystals (the interfacial structure of which is locally quite similar to that of linear polyelectrolytes).[26] On the other hand, the dynamic assumptions in the two-state-exchange model are physically unsound and must be replaced. This will be our main task in the present paper.

Until quite recently, counterion spin relaxation studies of polyelectrolyte solutions were confined to concentrated[27] systems. The general observation (excepting atypical polyelectrolytes such as poly(methacrylate) at low charge densities) is one of equal longtidudinal and transverse relaxation rates, indicative of short correlation times (for the fluctuating field gradient) as in simple electrolyte solutions. Under such conditions it is not possible to obtain detailed dynamic information about the processes that induce spin relaxation. The interpretation of the data has therefore emphasized static quantities, such as the fraction bound counterions,[24] and simplifying (often crude) assumptions about the dynamics have been introduced.

Improved NMR instrumentation has now made dilute polyelectrolyte solutions accessible to counterion relaxation studies. In an important contribution,[28] Levij, de Bleijser, and Leyte (hereafter referred to as LBL) reported extensive ^{23}Na counterion relaxation data from dilute solutions of poly(acrylate) and poly(styrenesulfonate). The results are dramatically different from those obtained from concentrated solutions. For dilute solutions the longitudinal and transverse relaxation rates are no longer equal and the transverse relaxation is biexponential. (Similar findings have been recorded independently, albeit in less detail, by others.[29]) The general indication from the relaxation data is one of a long ($\gg 10^{-9}$ s) correlation time which increases sharply upon dilution.[28] This behavior, which appears to be common to dilute solutions of all linear polyelectrolytes,[28] clearly demonstrates the deficiencies in the dynamic description of the two-state-exchange model. As yet, no theoretical explanation of these intriguing observations has been offered, except for a suggestion[28] that they are governed by the electrostatic persistence length of the polyion.

In the following we present a theory of counterion spin relaxation in dilute polyelectrolyte solutions, which gives a quantitative account of LBL's experimental data. In its present form, the theory is designed primarily to rationalize the anomalous relaxation behavior reported by LBL; i.e., it is a theory for the effect on the relaxation of the long-time tail of the total correlation function. (In a subsequent paper[30] we shall generalize the theory to include also the effect of the short-time behavior of the corelation function.) The theory is based on what may be termed a two-state mean-field model, which treats the equilibrium distribution and the dynamics of the counterions on an equal footing, recognizing that both are determined by the long-range Coulomb forces operating in polyelectrolyte solutions.

In the following section, we describe the physical model that we shall use to represent a polyelectrolyte solution and the interactions and dynamics therein that induce counterion spin relaxation. On the basis of this model, we then develop a theory for the spectral density function that determines the relaxation rates. Considerable simplification results from the assumption of time-scale separation for the molecular motions which govern the spectral density. The general formalism of this so-called two-step approximation is presented in Appendix B. The extension of the theory to include orientational correlation between neighboring polyions is given in Appendix C. We then apply the theory to LBL's ^{23}Na relaxation data.[28] In this connection we report some new data, the experimental conditions and methods of data acquisition and reduction of which are detailed in Appendix D. We discuss the possible effect on the counterion spin relaxation of a finite polyion persistence length and, in Appendix E, derive a correlation function for combined axial and radial counterion diffusion. Finally, we summarize the main conclusions of this work and indicate how the present theory may be extended.

Model

We consider counterion nuclear spins which are relaxed through the interaction of the nuclear electric quadrupole moment, eQ, with the fluctuating electric field gradient (efg) tensor, $\mathbf{V}(t)$, present at the nucleus.[25] This is the case for nearly all monatomic counterions of interest. We shall be concerned only with relaxation

(20) B. Lindman and S. Forsén, "Chlorine, Bromine and Iodine NMR. Physico-Chemical and Biological Applications", Springer-Verlag, Heidelberg, 1976.
(21) S. Forsén and B. Lindman in "Methods of Biochemical Analysis", Vol. 27, D. Glick, Ed., Wiley-Interscience, New York, 1980.
(22) S. Forsén and B. Lindman in "Annual Reports on NMR Spectroscopy", Vol. 11A, G. A. Webb, Ed., Academic Press, New York, 1981.
(23) R. M. Noyes, *J. Chem. Phys.*, **22** 1349 (1954).
(24) B. Lindman in "NMR of Newly Accessible Nuclei", Vol. 1, P. Laszlo, Ed., Academic Press, 1983, pp 193–231.
(25) A. Abragam, "The Principles of Nuclear Magnetism", Clarendon Press, Oxford, 1961.
(26) H. Wennerström, B. Lindman, G. Lindblom, and G. J. T. Tiddy, *J. Chem. Soc., Faraday Trans. 1*, **75**, 663 (1979).
(27) We use the terms "concentrated" and "dilute" according to wheter the polyion concentration is above or below ca. 0.1 monomol dm^{-3}. The definitions of various concentration regimes (dilute, semidilute, etc.), as they occur in polymer theory,[12] will not be used.
(28) M. Levij, J. de Bleijser, and J. C. Leyte, *Chem. Phys. Lett.*, **83**, 183 (1981).
(29) G. Gunnarsson and H. Gustavsson, *J. Chem. Soc., Faraday Trans. 1*, **78**, 2901 (1982).
(30) B. Halle and D. Y. C. Chan, to be submitted for publication.

in the motional narowing limit and in the absence of static quadrupolar perturbations. The relaxation behavior is then governed by the equilibrium time correlation function, $G(t)$, of the fluctuating efg[25]

$$G(t) = \langle V_0^L{}^*(0)\ V_0^L(t) \rangle \tag{1}$$

where V_0^L is the $m = 0$ spherical component, expressed in a lab-fixed frame (L), of the second-rank irreducible efg tensor, defined as in ref 31. In order to derive an expression for $G(t)$, we require a model which accounts for the origin of the efg and which identifies the molecular motions reponsible for its time dependence.

In a dilute solution of a symmetric electrolyte such as NaCl, the efg at the nucleus of a monatomic ion is due to instantaneous asymmetries in the surrounding solvent.[32-36] (By "asymmetry" we imply a point symmetry lower than $2 \times C_3$.) Recent Monte Carlo simulations[35,36] show that the efg is produced almost entirely by the water molecules in the primary coordination shell.

In a polyelectrolyte solution most counterions reside in the immediate vicinity of a polyion. Because of the highly asymmetric charge distribution between the species, the efg experienced by a counterion is expected to differ from that in a dilute solution of a symmetric electrolyte. There are two main differences. The first one is the direct contribution to the efg from the surrounding free charges associated with the polyion and with the other counterions. Since the efg from a point charge falls off with distance as r^{-3}, the overwhelming contribution comes from a few nearby charges. To describe this contribution accurately it is therefore essential to include the discrete nature of the polyion charge distribution, the electrostatic pair correlation between the counterions, and the finite size of the counterions. Several authors[37-39] have, nevertheless, evaluated the counterion efg within the primitive-model–PB approximation, in which the discrete polyion charges are replaced by a uniform surface charge density and in which the counterions are treated as uncorrelated point charges.[40] That this is indeed an invalid procedure is demonstrated by the finding[26] that the PB equation predicts quadrupolar line splittings (for counterions in macroscopically anisotropic systems) which are an order of magnitude smaller than those observed. Even more serious is the fact that the primitive-model–PB approximation predicts an efg tensor with a vanishing component along the polyion axis.[41] In a real polyelectrolyte solution, with discrete correlated charges, the charge distribution surrounding a counterion is not translationally invariant along the polyion axis. As we shall see this is a crucial point, since even a small axial efg component can dominate the counterion transverse relaxation provided that it fluctuates sufficiently slowly. [The PB approximation as applied to polyion systems yields a potential which is averaged over the positions of all N counterions in the system. However, to obtain the average efg experienced by a counterion one must average the instantaneous efg only over the positions of the remaining $N - 1$ counterions. This could be achieved by using a pair correlation function derived from the modified Poisson–Boltzmann equation.[42] That it is indeed inconsistent to identify the average (or root-mean-square) counterion efg with the second derivative of the PB potential is evident also from the fact that in such a procedure one has to assume the simultaneous validity of Laplace's and Poisson's equations.[37]]

The second main difference, as regards the counterion efg, between a polyelectrolyte solution and a dilute solution of a symmetric electrolyte is due to the perturbation of the primary hydration sheath around the counterion brought about by the polyion and nearby counterions. The free charges act here mainly through their associated electric field, rather than through their efg. However, non-Coulombic interactions with the polyion also contribute significantly.[26]

From what has been said, it is clear that an accurate theoretical evaluation of the counterion efg is a formidable task. (At present, the most promising approach to this problem is by way of computer simulations.) In the model presented here, we shall therefore regard the counterion efg as a free parameter. We do, however, assume that the perturbation of the efg is short-ranged, so that beyond a distance δ, of the order of a hydrated counterion diameter, from the polyion surface, the efg is essentially that of a dilute solution of a symmetric electrolyte. Due to the inherent local anisotropy of the molecular interactions within the perturbed region, the counterion efg principal axis system is not randomly oriented with respect to the polyion. As a consequence, complete randomization of the efg orientation cannot be achieved by the motions in the primary hydration sheath alone, as is the case in a dilute solution of a symmetric electrolyte. Additional motions are then required to average to zero the residual efg, which remains after partial averaging by motions in the hydration sheath.[31,43] As we shall see, the only motion that needs to be invoked in order to explain the anomalous relaxation in dilute polyelectrolyte solutions is the translational diffusion of the mobile counterions relative to the more sluggish polyions.

The behavior of the counterions will be described in terms of the cylindrical-cell model.[1-8] If the polyion contour length

$$L_c = Nl \tag{2}$$

where N is the degree of polymerization and l is the monomer length projected onto the polyion axis, is much greater than the cell radius, b, then we may neglect end effects and

$$b = (\pi l n_m)^{-1/2} \tag{3}$$

where n_m is the monomer number density. At the outset we also neglect any effects of a finite polyion persistence length; i.e., we take the cell to be an infinitely long, straight cylinder. (However, in a subsequent section we shall discuss end effects as well as persistence length effects.)

The interactions within the cell will be described in a primitive model, where the counterions (and any added salt) are treated as point charges immersed in a dielectric continuum of relative permittivity ϵ_r and where the polyion is represented by a cylinder of radius a with a uniform surface charge density

$$\sigma = -\alpha e/(2\pi a l) \tag{4}$$

where $-\alpha e$ is the average charge per monomer unit. Neglecting correlations between the mobile ions, we then obtain the PB equation for the mean potential, $\psi(r)$, in the cell

$$-\epsilon_0\epsilon_r \frac{1}{r}\frac{d}{dr}\left[r\frac{d\psi(r)}{dr}\right] = \sum_i z_i e n_i(b) \exp\left[-\frac{z_i e \psi(r)}{k_B T}\right] \tag{5a}$$

The sum runs over all species of mobile ions of valency z_i and local number density $n_i(r) \equiv n_i(b) \exp[-z_i e\psi(r)/(k_B T)]$. The boundary conditions are

$$\left.\frac{d\psi}{dr}\right|_a = -\frac{\sigma}{\epsilon_0\epsilon_r} \tag{5b}$$

$$\left.\frac{d\psi}{dr}\right|_b = 0 \tag{5c}$$

By convention we set $\psi(b) \equiv 0$. Equation 5 can be solved analytically if only counterions are present,[4-6] but in the presence of added salt one must resort to numerical methods.

(31) B. Halle and H. Wennerström, *J. Chem. Phys.*, **75**, 1928 (1981).
(32) H. G. Hertz, *Ber. Bunsenges. Phys. Chem.*, **77**, 531 (1973).
(33) H. L. Friedman in "Protons and Ions Involved in Fast Dynamic Phenomena", P. Laszlo, Ed., Elsevier, Amsterdam, 1978.
(34) J. T. Hynes and P. G. Wolynes, *J. Chem. Phys.*, **75**, 395 (1981).
(35) S. Engström and B. Jönsson, *Mol. Phys.*, **43**, 1235 (1981).
(36) S. Engström, B. Jönsson, and B. Jönsson, *J. Magn. Reson.*, **50**, 1 (1982).
(37) J. J. van der Klink, L. H. Zuiderweg, and J. C. Leyte, *J. Chem. Phys.*, **60**, 2391 (1974).
(38) A. Delville, H. Gilboa, and P. Laszlo, *J. Chem. Phys.*, **77**, 2045 (1982).
(39) A. Delville and P. Laszlo, *Biophys. Chem.*, **17**, 119 (1983).
(40) B. Jönsson, H. Wennerström, and B. Halle, *J. Phys. Chem.*, **84**, 2179 (1980).
(41) J. C. Leyte, *Chem. Phys. Lett.*, **66**, 417 (1979).
(42) S. Levine, C. W. Outhwaite, and L. B. Bhuiyan, *J. Electroanal. Chem.*, **123**, 105 (1981).
(43) H. Wennerström, G. Lindblom, and B. Lindman, *Chem. Scr.*, **6**, 97 (1974).

TABLE I: Typical Magnitudes of Some Properties of Dilute Polyelectrolyte Solutions[a]

c_m/(mol dm^{-3})	α	b/nm	$-ze\psi(a)/(k_BT)$	P	τ_{cell}/ns	τ_δ/ns
10^{-1}	1	4.598	5.298	0.4761	17.30	0.2321
10^{-2}	1	14.54	7.734	0.4245	270.0	0.2476
10^{-3}	1	45.98	10.11	0.4027	3411	0.2547
10^{-4}	1	145.4	12.46	0.3913	39150	0.2586
10^{-2}	0.5	14.54	5.716	0.1779	115.8	0.1423
10^{-2}	0	14.54	0	0.0036	26.34	0.06013

[a] All results pertain to monovalent counterions in the absence of added salt. Parameter values were as follows: T = 298.15 K, ϵ_r = 78.54, $D = 1 \times 10^{-9}$ m^2 s^{-1}, l = 0.25 nm, a = 0.5 nm, δ = 0.5 nm. The calculations are based on eq 3 and A5–A7. The mean counterion residence time in the perturbed region, τ_δ, is given by eq 13 if b is replaced by $a + \delta$ as the upper integration limits.

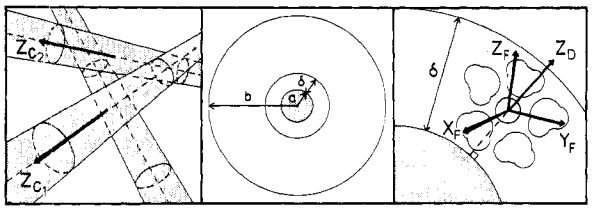

Figure 1. Neighboring polyions are orientationally correlated; i.e., the relative orientation of their cylinder axes (z_{C_1} and z_{C_2}) is nonrandom. Each polyion of radius a is centered in a cylindrical cell of radius b. Local motions in the hydration sheath partially average the efg (principal frame F) at a counterion nucleus. The local environment in the perturbed region ($a < r < a + \delta$) is anisotropic so that the residual efg is nonrandomly oriented with respect to the surface normal (z_D).

Two regions within the cell are defined by the dividing surface $r = a + \delta$, where δ is the previously discussed range of the polyion-induced counterion efg. The number of counterions, of the species whose NMR spectrum is being observed (superscript *), that reside within the perturbed region ($a < r < a + \delta$) is (per monomer)

$$2\pi l \int_a^{a+\delta} dr\, rn^*(r)$$

Hence, we get for the fraction, P, of such counterions that are in the perturbed region

$$P = \frac{2\pi l n^*(b)}{\alpha/z^* + \pi b^2 l n_s^*} \int_a^{a+\delta} dr\, r \exp\left[-\frac{z^* e\psi(r)}{k_BT}\right] \quad (6)$$

where n_s^* is the average number density of counterions (of the species whose NMR spectrum is being observed) which derive from added salt. Figure 1 illustrates some of the cell parameters introduced above.

It may be thought that the applicability of the cylindrical-cell model is restricted to hexagonal arrays of linear polyelectrolytes. However, it applies under far more general conditions. This is because a polyelectrolyte is a highly asymmetric electrolyte in which a counterion essentially experiences only the nearest polyion, the other ones being effectively screened. This assertion may be quantified by using the solution to the PB equation for a system containing several polyions.[44] We therefore believe that the cylindrical-cell model is appropriate over a wide range of polyion concentrations, even though the orientational correlation between neighboring polyions may vary within this concentration range. The normalized orientational pair correlation function for neighboring polyions (or cells) may be expanded in a Legendre basis

$$f(\theta_{C_1C_2}) = \sum_{l=0}^{\infty} (l + \tfrac{1}{2}) S_l P_l(\cos\theta_{C_1C_2}) \quad (7)$$

where $\theta_{C_1C_2}$ is the angle between two neighboring polyion axes (cf. Figure 1), P_l is the lth-degree Legendre polynomial, and S_l is the corresponding order parameter

$$S_l \equiv \int_{-1}^{1} dx\, f(x)\, P_l(x) \quad (8a)$$

The counterion spin relaxation is affected only by the second-rank order parameter

$$S_2 = \tfrac{1}{2}(3\langle\cos^2\theta_{C_1C_2}\rangle - 1) \quad (8b)$$

which we regard as a free parameter.

As in the description of the counterion distribution by the PB equation (eq 5a), we neglect all effects of correlations among the mobile ions on their dynamic behavior. Accordingly, we assume that the counterion translational diffusion is governed by the Smoluchowski mean-field diffusion equation[45,46]

$$\frac{1}{D^*}\frac{\partial}{\partial t} f^*(r,t) = \frac{1}{r}\frac{\partial}{\partial r} r\left[\frac{\partial}{\partial r} + \frac{d\phi^*(r)}{dr}\right] f^*(r,t) \quad (9)$$

Here $f^*(r,t)r\,dr$ is the probability of finding a "tagged" counterion to within dr of r at time t, subject to the appropriate initial condition. D^* is the counterion diffusion coefficient (as measured in a dilute solution of a symmetric electrolyte) and $\phi^*(r)$ is the reduced PB potential

$$\phi^*(r) \equiv \frac{z^* e}{k_BT}\psi(r) \quad (10)$$

As discussed in the following section, the long-time behavior of the correlation function is governed by the radial diffusion. Hence, the axial and azimuthal coordinates do not appear in eq 9. To further simplify the diffusion problem, we introduce what we call the dynamic cell approximation (DCA). According to the DCA, a counterion loses all correlation with a given polyion as soon as it reaches the cell boundary at $r = b$. (The accuracy of this approximation is discussed in the following section.) We impose a reflecting boundary at the polyion surface

$$\left.\frac{\partial f^*(r,t)}{\partial r}\right|_a + \left.\frac{d\phi^*}{dr}\right|_a f^*(a,t) = 0 \quad (11a)$$

while the cell boundary is taken, according to the DCA, to be absorbing

$$f^*(b,t) = 0 \quad (11b)$$

In the next section we show that the long-time behavior of the correlation function is determined by the mean residence time of a counterion in the cell, defined as

$$\tau_{cell} \equiv \int_0^{\infty} dt \int_a^b dr\, rf^*(r,t) \quad (12)$$

with the initial position averaged over the counterion equilibrium distribution. Direct integration of eq 9, using the boundary conditions 11, leads to[47]

$$\tau_{cell} = \frac{1}{D^*}\left[\int_a^b dr\, re^{-\phi^*(r)}\right]^{-1} \int_a^b dr\, \frac{1}{r} e^{\phi^*(r)} \left[\int_a^r ds\, se^{-\phi^*(s)}\right]^2 \quad (13)$$

In the absence of added salt, one can obtain analytical expressions for $\psi(r)$, P, and τ_{cell}. These are given in Appendix A. To give

(44) N. Imai and T. Ohnishi, *J. Chem. Phys.*, **30**, 1115 (1959); T. Ohnishi, N. Imai, and F. Oosawa, *J. Phys. Soc. Jpn*, **15**, 896 (1960).

(45) M. von Smoluchowski, *Ann. Phys. (Berlin)*, **48**, 1103 (1915).
(46) S. Chandrasekhar, *Rev. Mod. Phys.*, **15**, 1 (1943).
(47) N. S. Goel and N. Richter-Dyn, "Stochastic Models in Biology", Academic Press, New York, 1974.

TABLE II: Definition of Coordinate Systems

coordinate system	symbol	definition of z axis
laboratory frame	L	external static magnetic field
cell frame	C	local tangent to cell (and polyion) symmetry axis
director frame	D	local normal to cylindrical polyion surface
field gradient frame	F	principal axis corresponding to largest component of diagonal counterion efg tensor

an indication of the magnitudes of these quantities, we present in Table I results of some sample calculations.

Theory

Spin relaxation rates are in general determined by the values of the spectral density function, $J(\omega)$, at a few discrete frequencies. Neglecting effects of second-order frequency shifts,[48-50] we need to retain only the real part of the spectral density

$$J(\omega) = (eQ/h)^2 \int_0^\infty dt \cos(\omega t)\, G(t) \qquad (14)$$

with the efg correlation function $G(t)$ defined in eq 1. In order to separate contributions to $J(\omega)$ from various molecular degrees of freedom, we introduce four coordinate systems as defined in Table II and in Figure 1.

With the aid of the second-rank Wigner rotation matrix,[51] $\mathbf{D}^2(\Omega)$, we now transform the efg component $V_0^L(t)$, appearing in eq 1, from the L frame to its principal F frame, via the C and D frames

$$V_0^L(t) = \sum_m \sum_{m'} \sum_{m''} D^2_{0m}[\Omega_{LC}(t)]\, D^2_{mm'}[\Omega_{CD}(t)]\, D^2_{m'm''}[\Omega_{DF}(t)]\, V^F_{m''}[\Gamma(t)] \qquad (15)$$

where the sums run from -2 to $+2$. By means of these transformations, we have factorized the time dependence in $V_0^L(t)$ into four sets of stochastic variables: the three sets of Euler angles $\Omega_{LC}(t)$, $\Omega_{CD}(t)$, and $\Omega_{DF}(t)$ specifying the instantaneous relative orientation of the respective frames and the discrete-state variable $\Gamma(t)$. The random variable Γ has the effect of "switching on" different functions depending on the instantaneous position of the counterion: inside ($r < a + \delta$) or outside ($r > a + \delta$) the perturbed region.

The correlation function (1) is obtained by averaging over a joint equilibrium probability density and over a joint transition probability density. The former may be written

$$f(\Omega_{LC},\Omega_{CD},\Omega_{DF},\Gamma) = f(\Omega_{LC})\, f(\Omega_{CD})\, f(\Omega_{DF}|\Gamma)\, P(\Gamma) \qquad (16)$$

The Ω_{LC} factorization follows because all interactions within the cell are independent of its orientation. (Molecular degrees of freedom do not interact significantly with the external magnetic and gravitational fields.) The Ω_{CD} factorization is a consequence of the independence of the radial and azimuthal counterion distributions. However, the Ω_{DF} distribution depends on the state variable Γ as indicated in eq 16. From the overall isotropy of the system, it follows that

$$f(\Omega_{LC}) = 1/(8\pi^2) \qquad (17)$$

From the cylindrical symmetry of the cell it follows that

$$f(\Omega_{CD}) = (1/2\pi)\delta(\cos\theta_{CD})\, f(\phi_D) \qquad (18)$$

θ_{CD} is the angle ($\pi/2$) between the z_C and z_D axes.

To simplify the form of the joint transition probability we use to consider the characteristic time scales of the modulate the stochastic variables. We shall at the end-over-end reorientation of the polyion (and ate- l) as well as the translational diffusion of a the more or less curved polyion axis are both $_{LC}$ to remain essentially constant during the time that a given counterion remains in the cell. (These restrictions are lifted in the next section, where we show that polyion rotation can be important in dilute solutions of short polyions.) The only way in which Ω_{LC} can change is then by radial translational diffusion of the counterion over the cell boundary ($r = b$) and into another cell with a different orientation. The time scale for fluctuations in Ω_{LC} is thus set by the mean residence time of a counterion in the cell, τ_{cell}, as defined by eq 12.

The fluctuations in the Euler angles Ω_{DF} are due to motions in the primary hydration sheath and to other molecular motions occurring in the immediate neighborhood of the counterion. These motions proceed on a time scale of picoseconds.[35,36] The Euler angles Ω_{CD} are modulated by azimuthal translational diffusion of the counterion around the polyion on a time scale given roughly by $(a + \delta)^2/(4D)$, i.e., 10^{-10}–10^{-9} s. (Reorientation of the entire polyion around its axis is much slower and can safely be neglected.)

Finally, we consider the time scale for fluctuations in the state variable Γ. We do this with reference to Figure 2, in which we have plotted, for a typical case, the mean potential in the cell, the mean time, $\tau(a \to r)$, taken for a counterion, starting at the polyion surface, to reach the radial coordinate r for the first time, and the reencounter probability, $P(r \to a)$, i.e., the probability that a counterion, starting at r, reaches the polyion surface ($r = a$) before it reaches the cell boundary ($r = b$). The latter quantity is given by[47]

$$P(r \to a) = \left[\int_a^b ds\, \frac{1}{s} e^{\phi^*(s)}\right]^{-1} \int_r^b ds\, \frac{1}{s} e^{\phi^*(s)} \qquad (19)$$

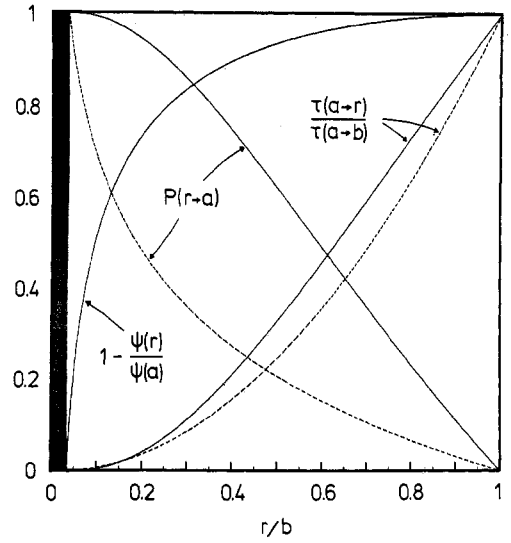

Figure 2. Some characteristics of the cylindrical-cell model of polyelectrolyte solutions. Shown as functions of the reduced radial cell coordinate, r/b (the polyion surface is at $r/b = a/b = 0.0344$), are (1) the mean electrostatic potential, in the reduced form $1 - \psi(r)/\psi(a)$, (2) the probability, $P(r \to a)$, that a counterion, which starts at r, reaches the polyion surface ($r = a$) before it reaches the cell boundary ($r = b$), and (3) the mean time, $\tau(a \to r)$, for a counterion, initially at the polyion surface, to reach the radial coordinate r for the first time, reduced by the corresponding time $\tau(a \to b)$. The solid curves were computed with the following parameter values: $T = 298.15$ K, $\epsilon_r = 78.54$, $z = 1$, $\alpha = 1$, $l = 0.25$ nm, $a = 0.50$ nm, $c_m = 0.01$ mol dm^{-3} and no added salt. The dashed curves correspond to free diffusion ($z = 0$).

The curves in Figure 2 reveal an important, and perhaps counterintuitive, fact: although counterions in the neighborhood of a polyion experience a very strong inward force (cf. the slope of the potential curve), they make substantial radial excursions

(48) R. Poupko, A. Baram, and Z. Luz, *Mol. Phys.*, **27**, 1345 (1974).
(49) L. G. Werbelow and A. G. Marshall, *J. Magn. Reson.*, **43**, 443 (1981).
(50) P.-O. Westlund and H. Wennerström, *J. Magn. Reson.*, **50**, 451
Brink and G. R. Satchler, "Angular Momentum", 2nd ed., ss, Oxford, 1968.

on a very short time scale. (Cf. also the last column of Table I.) The high reencounter probability near the polyion implies that a counterion makes many such excursions before it reaches the cell boundary and eventually escapes. In the free-diffusion case, reencounters occur less frequently so that a particle starting at $r = a$ reaches any $r > a$ faster than it would have done in the presence of the PB potential.

Let $P(t)$ be the probability of finding a counterion in the perturbed region $a < r < a + \delta$ at time t, given that it was there initially. Obviously, $P(t\rightarrow\infty) = P$, as given by eq 6. Now the state variable $\Gamma(t)$ is randomized on the time scale on which $P(t)$ evolves toward P. But from Figure 2 we can infer that the relatively fast radial excursions within the inner part of the cell suffice to bring $P(t)$ very close to its equilibrium value P. A quasi-steady-state situation then obtains within the cell, with the "tagged" counterions (those that started out in the perturbed state) being nearly Boltzmann distributed when they begin to slowly leak out of the cell through the absorbing boundary at $r = b$. The fluctuations in $\Gamma(t)$ thus occur essentially on a time scale which is short compared to the characteristic time, τ_{cell}, for fluctuations in Ω_{LC}. This steady-state approximation, i.e., the Γ–Ω_{LC} time-scale separation, is very accurate when the counterion distribution is distinctly inhomogeneous.[30]

From what has been said it is clear that, in a dilute polyelectrolyte solution, Ω_{LC} fluctuates much more slowly than the remaining stochastic variables Ω_{CD}, Ω_{DF}, and Γ. As a consequence of this time-scale separation, the joint transition probability density factorizes as

$$f(\Omega_{LC},\Omega_{CD},\Omega_{DF},\Gamma;t|\Omega^0_{LC},\Omega^0_{CD},\Omega^0_{DF},\Gamma^0) = f(\Omega_{LC};t|\Omega^0_{LC})\, f(\Omega_{CD},\Omega_{DF},\Gamma;t|\Omega^0_{CD},\Omega^0_{DF},\Gamma^0) \quad (20)$$

where a superscript zero denotes the initial value of the respective variable.

Because of the time-scale separation, it is convenient to divide $V^L_0(t)$ into two parts as

$$V^L_0(t) = V^L_{0f}(t) + V^L_{0s}(t) \quad (21a)$$

with

$$V^L_{0f}(t) \equiv V^L_0(t) - V^L_{0s}(t) \quad (21b)$$

$$V^L_{0s}(t) \equiv \int d\Omega_{CD}\, f(\Omega_{CD}) \sum_\Gamma P(\Gamma) \int d\Omega_{DF}\, f(\Omega_{DF}|\Gamma)\, V^L_0(t) \quad (21c)$$

The averaging in eq 21c over the rapidly fluctuating variables ensures that $V^L_{0s}(t)$ contains only the slow time dependence associated with Ω_{LC}.

Because of the statistical independence of the fast and slow variables, as expressed by eq 20, the cross-correlations between V^L_{0f} and V^L_{0s} vanish and the correlation function 1 may be written as the following sum

$$G(t) = G_f(t) + G_s(t) \quad (22)$$

where the two terms involve $V^L_{0f}(t)$ and $V^L_{0s}(t)$, respectively. Equation 22, which is derived more formally in Appendix B, constitutes the vital part of the two-step model, previously developed for use in connection with spin relaxation of ions[43] and water[31] in colloidal and polyelectrolyte systems.

If eq 22 is inserted into eq 14, we obtain the corresponding decomposition of the spectral density

$$J(\omega) = J_f(\omega) + J_s(\omega) \quad (23)$$

Now quadrupolar relaxation rates are determined by the values of $J(\omega)$ at $\omega = 0$, ω_0, and $2\omega_0$, where ω_0 is the Larmor frequency.[25] Typically, ω_0 is 10^8–10^9 rad s^{-1}. It is clear from eq 14 that $J(\omega)$ is frequency dependent only around frequencies such that $1/\omega$ falls on the time scale where $G(t)$ decays. We shall assume that all the fast motions are fast relative to $1/\omega_0$, whereas the slow motions are slow relative to $1/\omega_0$. Then

$$J_f(0) = J_f(\omega_0) = J_f(2\omega_0) \equiv J_f \quad (24a)$$

$$J_s(0) = (eQ/h)^2 \int_0^\infty dt\, G_s(t) \quad (24b)$$

$$J_s(\omega_0) = J_s(2\omega_0) = 0 \quad (24c)$$

In the remainder of this section we shall be concerned only with $J_s(0)$.

When $V^L_0(t)$ from eq 15 is inserted into eq 21c, we obtain

$$V^L_{0s}(t) = \sum_m D^2_{0m}[\Omega_{LC}(t)] \sum_{m'} \int d\Omega_{CD}\, f(\Omega_{CD})\, D^2_{mm'}(\Omega_{CD}) \times \sum_\Gamma P(\Gamma) \int d\Omega_{DF}\, f(\Omega_{DF}|\Gamma) \sum_{m''} D^2_{m'm''}(\Omega_{DF})\, V^F_{m''}(\Gamma) \quad (25)$$

It follows from eq 18 that

$$\int d\Omega_{CD}\, f(\Omega_{CD})\, D^2_{mm'}(\Omega_{CD}) = \delta_{m0} \langle D^2_{0m'}(\Omega_{CD})\rangle \quad (26)$$

with $\langle D^2_{00}(\Omega_{CD})\rangle = d^2_{00}(\pi/2) = -1/2$. Hence, we may write

$$V^L_{0s}(t) = -\tfrac{1}{2} D^2_{00}[\Omega_{LC}(t)] \sum_\Gamma P(\Gamma)\, \bar{V}(\Gamma) \quad (27)$$

where we have introduced the residual efg, $\bar{V}(\Gamma)$, that remains after statistical averaging over Ω_{DF} and ϕ_D in state Γ

$$\bar{V}(\Gamma) \equiv \sum_m \frac{\langle D^2_{0m}(\Omega_{CD})\rangle}{\langle D^2_{00}(\Omega_{CD})\rangle} \int d\Omega_{DF}\, f(\Omega_{DF}|\Gamma) \sum_{m'} D^2_{mm'}(\Omega_{DF})\, V^F_{m'}(\Gamma) \quad (28)$$

If there were at least threefold symmetry with respect to the director, as for a planar interface, then only the $m = 0$ term would survive in eq 28. In the unperturbed state ($r > a + \delta$), $f(\Omega_{DF}) = 1/(8\pi^2)$ by definition, so that $\bar{V} = 0$. Hence, only the perturbed state contributes to the sum in eq 27 and we get

$$V^L_{0s}(t) = -\tfrac{1}{2} P \bar{V}_\delta D^2_{00}[\Omega_{LC}(t)] \quad (29)$$

where P is the fraction of counterions in the perturbed state, as given by eq 6, and where the subscript δ denotes the perturbed state.

When $V^L_{0s}(t)$ from eq 29 is inserted into eq 24b, we get

$$J_s(0) = (3/40)(P\bar{\chi}_\delta)^2 \int_0^\infty dt\, \tilde{G}_s(t) \quad (30)$$

where we have defined an averaged quadrupole coupling constant[25,31]

$$\bar{\chi}_\delta \equiv \frac{2}{6^{1/2}} \frac{eQ\bar{V}_\delta}{h} \quad (31)$$

and a reduced correlation function

$$\tilde{G}_s(t) \equiv \langle D^2_{00}[\Omega_{LC}(0)]\, D^2_{00}[\Omega_{LC}(t)]\rangle / \langle [D^2_{00}(\Omega_{LC})]^2\rangle \quad (32)$$

The extra factor $1/5$ in eq 30 comes from $\langle [D^2_{00}(\Omega_{LC})]^2\rangle = 1/5$, by virtue of eq 17 and the orthogonality of the D elements.[51]

Now we have assumed that the only way that Ω_{LC} can change is by translational diffusion of the counterion from one polyion to another. If the polyions are completely uncorrelated in orientation, i.e., if the polyion order parameter $S_2 = 0$ (cf. eq 8b), then $\tilde{G}_s(t)$ is simply the probability that the counterion at time t resides in the same cell as it did initially. If we, furthermore, invoke the DCA, as described in the previous section, then $\tilde{G}_s(t)$ is given by the probability that the counterion has not yet reached the cell boundary, i.e.

$$\tilde{G}_s(t) = \int_a^b dr\, r f^*(r,t) \quad (33)$$

where $f^*(r,t)$ is the solution to eq 9 subject to the boundary conditions 11. On combining eq 12, 30, and 33, we arrive at the simple result

$$J_s(0) = (3/40)(P\bar{\chi}_\delta)^2 \tau_{cell} \quad (34)$$

Note that, since only the zero-frequency spectral density is required, we do not have to make any assumptions about the functional form (e.g., exponential) of $\tilde{G}_s(t)$.

Even for highly charged polyions, the PB potential is quite flat in the neighborhood of the midpoint between two polyions (cf. Figure 2). Diffusional trajectories whereby a counterion crosses

the cell boundary at $r = b$ and shortly thereafter recrosses it on its return to the original cell should therefore occur quite frequently. The neglect of such trajectories is clearly a deficiency in the DCA. By studying the behavior of the spectral density as the absorbing boundary is successively displaced toward larger r (outside the cell boundary), it can be shown[30] that such cell boundary recrossings contribute almost exactly a factor of 2 to $J_s(0)$. For highly charged polyions, this factor of 2 is associated almost exclusively with the increased correlation time for radial counterion diffusion. Introducing this ad hoc improvement of the DCA into eq 34, we may write

$$J_s(0) = (3/40)(P\bar{\chi}_\delta)^2\tau_{rad} \quad (35)$$

where we have defined

$$\tau_{rad} \equiv 2\tau_{cell} \quad (36)$$

with τ_{cell} defined, as before, be eq 12.

In Appendix C we generalize eq 35 to include orientational correlation between the polyions. The result is

$$J_s(0) = (3/40)(P\bar{\chi}_\delta)^2\tau_{rad}/(1 - S_2) \quad (37)$$

where S_2 is defined by eq 8b. The final result for the spectral density values required to calculate the relaxation rates now follows from eq 23, 24, and 37

$$J(0) = J_f + (3/40)(P\bar{\chi}_\delta)^2\tau_{rad}/(1 - S_2) \quad (38a)$$

$$J(\omega_0) = J(2\omega_0) = J_f \quad (38b)$$

Applications

We are now ready to confront the model and the theory, as presented in the two previous sections, with experimental fact. For this purpose, we use the extensive data on ^{23}Na transverse relaxation in dilute polyelectrolyte solutions reported by LBL.[28] For a nucleus, like ^{23}Na, with spin quantum number $I = {}^3/_2$, the transverse magnetization decays, in general, biexponentially with relaxation rates given by[25,52]

$$R_2^+ = (2\pi^2/3)[J(0) + J(\omega_0)] \quad (39a)$$

$$R_2^- = (2\pi^2/3)[J(\omega_0) + J(2\omega_0)] \quad (39b)$$

and with the spectral density function, $J(\omega)$, defined by eq 14. For very long correlation times, as might possibly occur in extremely dilute salt-free polyelectrolyte solutions, these expressions are no longer valid. The failure of eq 39a is due to the breakdown of the motional narrowing condition[25] ($\omega_Q\tau_c \ll 1$, where ω_Q is the quadrupolar interaction, in frequency units, fluctuating with a correlation time τ_c), while eq 39b should include a contribution from a second-order frequency shift.[50]

The intriguing and hitherto not satisfactorily explained counterion relaxation behavior in polyelectrolyte solutions is contained in the difference

$$\Delta R_2 \equiv R_2^+ - R_2^- = (2\pi^2/3)[J(0) - J(2\omega_0)] \quad (40)$$

On substitution of eq 38, we get

$$\Delta R_2 = (\pi^2/20)P^2(\bar{\chi}_\delta)^2\tau_{rad}/(1 - S_2) \quad (41)$$

TABLE III: Parameter Values Used in All Calculations

T	294.45 K
ϵ_r	79.88
D	1.22×10^{-9} m^2 s^{-1}
l	0.25 nm
δ	0.50 nm
a(NaPAA)	0.30 nm
a(NaPSS)	0.50 nm

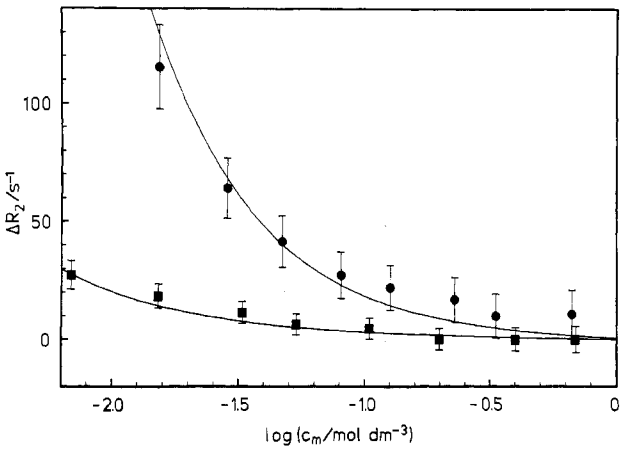

Figure 3. ΔR_2 vs. polyelectrolyte monomolarity for NaPAA, $N = 27780$, $\alpha = 0.89$ (●) and $\alpha = 0.49$ (■). The experimental data were taken from ref 28 and the curves were calculated from eq 41 with $\bar{\chi}_\delta(1 - S_2)^{-1/2} = 71$ kHz and the parameter values of Table III.

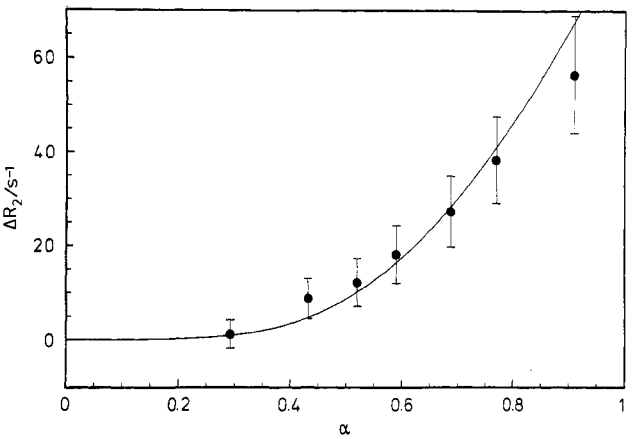

Figure 4. ΔR_2 vs. degree of dissociation for NaPAA, $N = 27780$, $c_m = 3.03 \times 10^{-2}$ mol dm^{-3}. The experimental data were taken from ref 28 and the curve was calculated from eq 41 with $\bar{\chi}_\delta(1 - S_2)^{-1/2} = 71$ kHz and the parameter values of Table III.

In the absence of added salt, P and τ_{cell} are given analytically by eq A6 and A7, respectively. In the presence of added salt, these quantities are obtained from eq 6 and 13 together with the numerical solution of the Poisson–Boltzmann equation.[5]

We stress that eq 41 contains only one adjustable parameter, viz., the composite quantity $\bar{\chi}_\delta(1 - S_2)^{-1/2}$. As independent estimates of $\bar{\chi}_\delta$ are available (vide infra), it is thus in principle possible to extract from the relaxation data some information about polyelectrolyte solution structure in terms of the second-rank orientational order parameter S_2. The parameter values used in all calculations of P and τ_{cell} are listed in Table III. The use of different values for these parameters, within physically reasonable limits (±0.005 nm for l, ±0.2 nm for a and δ), might change the deduced $\bar{\chi}_\delta(1 - S_2)^{-1/2}$ by up to 30%, whereas the goodness of the fits would remain virtually unaffected. The parameters in Table III are all treated as constants with respect to variations in polyion concentration and charge density and in added-salt concentration.

Figures 3 and 4 show the fits of eq 41 to the NaPAA data. Only one parameter, $\bar{\chi}_\delta(1 - S_2)^{-1/2} = 71$ kHz, was adjusted in computing the three theoretical curves, which all fall within the experimental

(52) P. S. Hubbard, *J. Chem. Phys.*, **53**, 985 (1970).
(53) G. Lindblom, B. Lindman, and G. J. T. Tiddy, *J. Am. Chem. Soc.*, **100**, 2299 (1978).
(54) P. Ekwall, L. Mandell, and K. Fontell, *Acta Chem. Scand.*, **22**, 1543 (1968).
(55) I. D. Leigh, M. P. McDonald, R. M. Wood, G. J. T. Tiddy, and M. A. Trevethan, *J. Chem. Soc., Faraday Trans. 1*, **77**, 2867 (1981).
(56) F. Husson, H. Mustacchi, and V. Luzzati, *Acta Crystallogr.*, **13**, 668 (1960).
(57) H. Gustavsson, G. Lindblom, B. Lindman, N. O. Persson, and H. Wennerström in "Liquid Crystals and Ordered Fluids" Vol. II, J. F. Johnson and R. S. Porter, Eds., Plenum Press, New York, 1974.
(58) K. Fontell, *J. Colloid Interface Sci.*, **44**, 318 (1973).
(59) H. T. Edzes, A. Rupprecht, and H. J. C. Berendsen, *Biochem. Biophys. Res. Commun.*, **46**, 790 (1972).

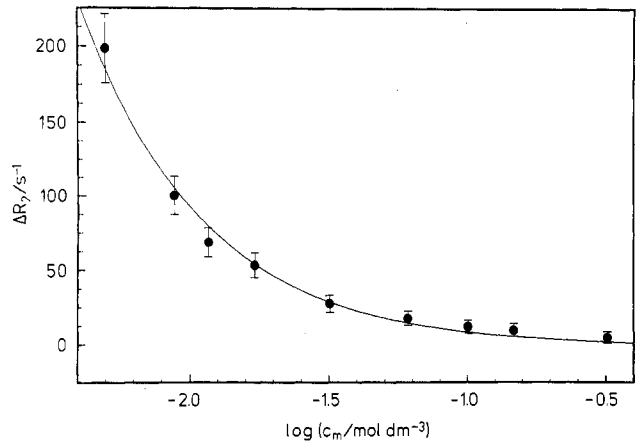

Figure 5. ΔR_2 vs. polyelectrolyte monomolarity for NaPSS, $N = 1070$, $\alpha = 0.81$. The experimental data were taken from ref 28 and the curve was calculated from eq 41 with $\bar{\chi}_\delta(1 - S_2)^{-1/2} = 71$ kHz and the parameter values of Table III.

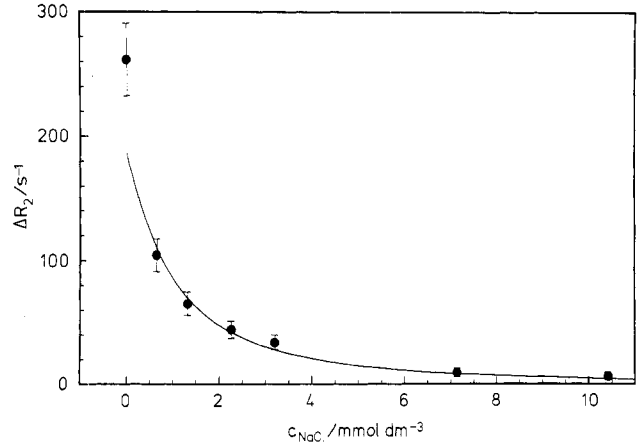

Figure 6. ΔR_2 vs. NaCl molarity for NaPSS, $N = 3155$, $\alpha = 0.70$, $c_m = 4.9 \times 10^{-3}$ dm^{-3}. The experimental data were taken from ref 28 and the curve was calculated from eq 41 with $\bar{\chi}_\delta(1 - S_2)^{-1/2} = 88$ kHz and the parameter values of Table III.

uncertainty as quoted by LBL.[28] Similar agreement was obtained for the dilution experiment on NaPSS (degree of polymerization, $N = 1070$), as shown in Figure 5. As in the case of NaPAA, the adjusted parameter value is $\bar{\chi}_\delta(1 - S_2)^{-1/2} = 71$ kHz.

Figure 6 shows the fit to the data form the NaCl-addition experiment on NaPSS ($N = 3155$), which yielded the somewhat higher value $\bar{\chi}_\delta(1 - S_2)^{-1/2} = 88$ kHz. Again the agreement is quantitative, except for the point at zero salt concentration. We believe that this disagreement is due to an experimental error. This point, with $R_2^+ = 290$ s^{-1}, is by far the largest relaxation rate reported by LBL.[28] For such rapid decays, instrumental factors (e.g., spectrometer dead time) might produce systematic errors in the measurements. Furthermore, the zero-salt measurement in Figure 6 is not consistent with the zero-salt data in Figure 5. This measurement was made at nearly the same polyelectrolyte concentration as the lowest concentration point in Figure 5, the main difference being the lower α value. (On the basis of LBL's data,[28,60] we expect no N dependence between Figures 5 and 6.) With the parameters that gave the excellent fit in Figure 5, but with $\alpha = 0.70$, we calculate a ΔR_2 value which is lower than that reported by LBL (the zero-salt point in Figure 6) by about a factor of 2.

TABLE IV: Residual ^{23}Na Quadrupole Coupling Constant, $\bar{\chi}_\delta$, for Na^+ at Interfaces in Various Lyotropic Liquid Crystals and in Oriented DNA[a]

system	$-\sigma$/C m^{-2}	$\bar{\chi}_\delta$/ kHz	ref
$C_8SO_4Na-C_{10}OH-H_2O$ (lamellar phase)	0.28	60	53, 54
$C_8SO_3Na-C_{10}OH-H_2O$ (lamellar phase)	0.28	60	53
$C_{12}SO_4Na-D_2O$ (lamellar phase)	0.38	77	55, 56
$C_{12}SO_4Na-D_2O$ (hexagonal phase)	0.28	79	55, 56
Aerosol OT–H_2O (lamellar phase)	0.25	135	57, 58
$C_7COONa-C_{10}OH-H_2O$ (lamellar phase)	0.19	35	53, 54
monooctanoin–H_2O–NaCl (lamellar phase)	0	40	53
NaDNA–H_2O–NaCl (oriented)	0.15	52	59

[a] These $\bar{\chi}_\delta$ values have been derived from quadrupolar line splittings in the ^{23}Na NMR spectrum. According to the two-state model, the splitting is $\Delta = P\bar{\chi}_\delta/4$ for planar symmetry and $\Delta = P\bar{\chi}_\delta/8$ for cylindrical symmetry.[43] (These formulas pertain to polycrystalline samples and to samples oriented perpendicular to the magnetic field.) The fraction, P, of Na^+ ions that reside within the perturbed region (extending a distance δ from the charged surface) was calculated from eq 6 or its planar-symmetry equivalent and the appropriate solution of the Poisson–Boltzmann equation with $\delta = 0.5$ nm. Geometric parameters were taken from X-ray data (cf. references given in the table).

The quantitative agreement between theory and experiment, as demonstrated in Figures 3–6, implies that the quantity $\bar{\chi}_\delta(1 - S_2)^{-1/2}$ is essentially independent of polyion concentration, polyion charge, and salt concentration—at least within the investigated ranges of these variables. If $S_2 \ll 1$, then the relaxation behavior is practically independent of S_2 (a variation in which may then pass unnoticed) and no information can be extracted about the orientational pair correlation between the polyions. The observed invariance then refers to the residual ^{23}Na quadrupole coupling constant, $\bar{\chi}_\delta$, averaged by local motions in the perturbed region.

The deduced values (71 and 88 kHz) for the polyelectrolyte solutions fall within the range of $\bar{\chi}_\delta$ values obtained from ^{23}Na quadrupole line splittings in macroscopically anisotropic systems such as lyotropic liquid crystals. Some typical results are shown in Table IV. Because of the symmetry difference between a cylindrical and a planar interface, the corresponding residual efg's are expected to differ somewhat. Thus, the additional ϕ_D averaging at the cylindrical interface should reduce $\bar{\chi}_\delta$ relative to its value for the corresponding flat surface. (The ϕ_C averaging, brought about by counterion diffusion around the polyion rod, is explicitly accounted for by the factor $-1/2$ in eq 27. However, this effect is probably quite small and obscured by differences in the molecular details of the interactions at the interfaces. The invariance of $\bar{\chi}_\delta$ with respect to polyion and salt concentration is in accord with conclusions from studies[26,53,55,57] of quadrupolar line splittings. The invariance of $\bar{\chi}_\delta$ with respect to polyion charge (or α) fits in well with the lack of correlation between $\bar{\chi}_\delta$ and the surface charge density, as evidenced by the data in Table IV, and supports our notion that the efg at an ionic nucleus is due primarily to local short-range interactions.

In a subsequent paper,[60] LBL report further ^{23}Na relaxation measurements on NaPSS solutions at very low polyion concentrations. The dramatic rise in R_2^+ upon dilution (cf. Figures 3 and 5) was found to stop at about 10^{-3} mol dm^{-3} only to be followed, on further dilution, by an equally dramatic decline. At the lowest concentrations studied (just below 10^{-4} mol dm^{-3}) R_2^+ has nearly merged with R_2^-, indicating that the effective correlation

(60) M. Levij, J. de Bleijser, and J. C. Leyte, *Chem. Phys. Lett.*, **87**, 34 (1982).
(61) V. Vlachy and D. Dolar, *J. Chem. Phys.*, **76**, 2010 (1982).
(62) F. Perrin, *J. Phys. Radium*, **5**, 497 (1934).
(63) T. Odijk, *J. Polym. Sci., Polym. Phys. Ed.*, **15**, 477 (1977).
(64) J. Skolnick and M. Fixman, *Macromolecules*, **10**, 944 (1977).
(65) S. Lifson and J. L. Jackson, *J. Chem. Phys.*, **36**, 2410 (1962).
(66) P. J. Flory, "Statistical Mechanics of Chain Molecules", Interscience, New York, 1969.
(67) M. Abramowitz and I. A. Stegun, "Handbook of Mathematical Functions", Dover, New York, 1965.
(68) G. Pólya, *Math. Ann.*, **84**, 149 (1921).
(69) M. Benmouna, G. Weill, H. Benoit, and Z. Akcasu, *J. Phys. (Paris)*, **43**, 1679 (1982).

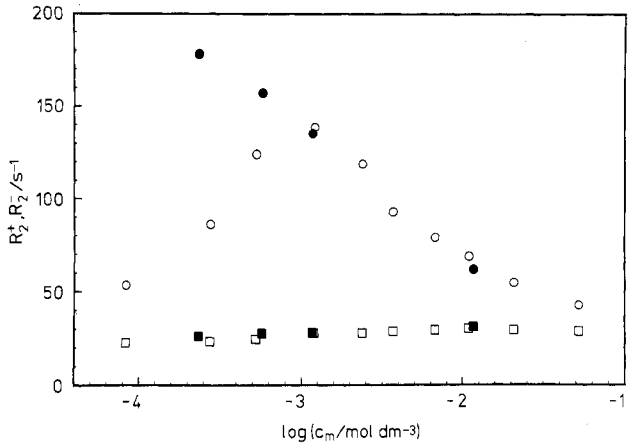

Figure 7. Transverse relaxation rates (circles for R_2^+, squares for R_2^-) vs. NaPSS monomolarity. Open symbols refer to data taken from ref 60 (N = 170, α = 0.90, T = 25 °C, ν_0 = 66.1 MHz) and filled symbols refer to our data (N = 180, α = 0.88, T = 20 °C, ν_0 = 51.9 MHz).

time has decreased to about 10^{-9} s. This behavior is quite unexpected—indeed, it cannot be rationalized within the framework of the present relaxation theory and the current knowledge about polyelectrolyte solutions. For this reason we undertook a reinvestigation of the concentration dependence of the ^{23}Na transverse relaxation rates in NaPSS solution. The experimental conditions and method of data reduction are detailed in Appendix D, and in Figure 7 we compare our results with those of LBL.[60] The agreement between the two sets of experiments is excellent, except for R_2^+ below 10^{-3} mol dm^{-3}, where our data show a continuing rise of R_2^+ with dilution. It is our belief, therefore, that the sharp decline in R_2^+ below 10^{-3} mol dm^{-3} reported by LBL[60] is an experimental artifact. It may be noted that a fixed trace amount of salt (divalent cations in particular) could reduce R_2^+ considerably at these low polyion concentrations, more so as the solution is diluted.[70]

There remains one experimental observation to be explained, namely, the dependence of ΔR_2 on the degree of polymerization, N, of the polyion. This dependence was studied by LBL[28,60] for NaPSS solutions for which they reported large effects, e.g., $\Delta R_2(N{=}1070)/\Delta R_2(N{=}87) \approx 11$ at a polyelectrolyte concentration of 5×10^{-3} mol dm^{-3}. Up to this point we have neglected end effects and calculated P and τ_{cell} for an infinitely long, straight cylindrical cell. However, as the cell diameter, $2b$, becomes of the same order of magnitude as the polyion contour length, L_c, the cylindrical-cell model breaks down. This is indeed the case in some of LBL's experiments: for 5×10^{-3} mol dm^{-3} NaPSS of N = 87 we find, from eq 2 and 3, L_c = 22 nm and $2b$ = 41 nm.

A simple ad hoc extension of the model, to incorporate some effects of a finite N, is to put hemispherical end caps on the cylindrical cell. For given n_m and N, such a cell has a smaller radius than an infinitely long cell. Equation 3 is replaced by

$$b = [\pi l n_m(1 + 4b/(3Nl))]^{-1/2} \quad (42)$$

In the aforementioned case the cell diameter is reduced from 41 to 30 nm. This has very little effect on P, but it does reduce τ_{cell} by about a factor of 2, which, however, falls short of the observed factor of 11.

To obtain a more realistic description of end effects, we must recognize that the hemispherical caps contribute a substantial fraction of the cell volume and that a diffusing counterion therefore has a good chance of leaving the cell through the caps rather than through the cylindrical surface. We shall not here embark on the nontrivial numerical exercise of solving the Poisson–Boltzmann and Smoluchowski equations for a hemisphere-capped cylindrical cell. It is clear, however, that the entropic effect of the increased spatial dimensionality at the ends of the cell must be to reduce P as well as τ_{cell}. In fact, the reduction in P with decreasing N has recently been verified through Monte Carlo simulations.[61] Furthermore, we have performed calculations on a spherical cell, which is appropriate for describing the potential far from the polyion in the limit $b \gg L_c$, demonstrating that the effect may be substantial. Hence, it seems reasonable to ascribe the observed N dependence in ΔR_2 to the increasing cell dimensionality (from 2 toward 3) that accompanies dilution of a finite polyion.

Another source of N dependence in ΔR_2 is the appearance, for short polyions, of an additional motional degree of freedom that can modulate the residual efg. A possible candidate is the end-over-end rotation of the entire polyion (and cell). Equation 41 should then have $\tau_{rad}/(1 - S_2)$ replaced by an effective correlation time, τ_{eff}, given by

$$1/\tau_{eff} = (1 - S_2)/\tau_{rad} + 1/\tau_{rot} \quad (43)$$

where we have assumed that the radial and rotational correlation functions decay exponentially (cf. Appendix E). If the polyion can be described as a rigid rod, then the rotational correlation time is[62]

$$\tau_{rot} = \pi\eta L_c^3/\{9k_BT[2 \ln (L_c/a) - 1]\} \quad (44)$$

where η is the shear viscosity of the solvent. For NaPSS of N = 87 eq 44 yields τ_{rot} = 135 ns, to be compared with τ_{rad} = 408 ns ($c_m = 5 \times 10^{-3}$ mol dm^{-3}, α = 0.90 and b from eq 42). Although this value for τ_{rad} is an upper limit (vide supra), it appears likely that, for such short polyions, end-over-end rotation begins to affect the relaxation behavior at polyion concentrations in the millimolar range. On progressive dilution of the polyelectrolyte solution, τ_{rot} should eventually take over completely, thereby causing ΔR_2 to level off. In the experiments of Figure 7, this should occur at about 10^{-5} mol dm^{-3}.

In the preceding we have taken the cylindrical cell to be straight; i.e., we have assumed an infinite persistence length, L_p, for the polyion. A finite persistence length introduces the possibility of modulation of the residual, locally averaged efg through axial counterion diffusion along the curved polyion. In Appendix E we show that the effective correlation time for combined radial and axial counterion diffusion is given by

$$1/\tau_{eff} = (1 - S_2)/\tau_{rad} + 1/(2\tau_{rad}\tau_{axi})^{1/2} \quad (45)$$

where

$$\tau_{axi} = L_p^2/2D \quad (46)$$

The persistence length of a polyion is determined by the electrostatic repulsion, partially screened by the counterions and any added salt, between segments of the polyion chain. (We neglect the small nonelectrostatic contribution, of order 10^{-9} m, to L_p.) For a line charge whose segments interact via a Debye–Hückel potential, one has in the absence of added salt[63,64]

$$L_p = \alpha/(16\pi l^2 n_m) \quad (47)$$

Recently, the electrostatic persistence length has been calculated also by way of numerical solutions of the nonlinear PB equation for a curved polyion of finite cylinder radius in the cell model[10] and in an infinite reservoir of added salt.[10,11] Whereas eq 47 does not contain the polyion radius a, the PB results turn out to be quite sensitive to this parameter. In the absence of added salt and in the polyion concentration range of interest here, the linear theory, eq 47, predicts shorter persistence lengths than does the PB theory.[10] The discrepancy is about a factor of 3 for NaPSS (a = 0.5 nm) and nearly an order of magnitude for NaPAA (a = 0.3 nm). Unfortunately, currently available experimental data do not allow an unambiguous assessment of the accuracy of these theories.[9]

In Table V we present some numerical estimates of τ_{axi} and τ_{eff} based on the two theories for L_p. Judging from the PB results,

(70) After the submission of this paper, we received confirmation from Dr. J. C. Leyte that the decline in R_2^+ below 10^{-3} mol dm^{-3}, as reported in ref 60, is indeed an artifact. It appears to be due to the slow release of ions from the Wilmad-513-1PP sample tubes that were used (J. C. Leyte, personal communication).

TABLE V: Polyion Persistence Length and Axial Counterion Diffusion[a]

c_m/ mol dm^{-3}	L_p theory	L_p/m	τ_{axi}/s	τ_{rad}/s	τ_{eff}/s
10^{-1}	DH	5.3×10^{-9}	1.2×10^{-8}		1.3×10^{-8}
	PB	2.5×10^{-8}	2.5×10^{-7}	2.8×10^{-8}	2.3×10^{-8}
10^{-2}	DH	5.3×10^{-8}	1.2×10^{-6}		3.1×10^{-7}
	PB	1.8×10^{-7}	1.3×10^{-5}	4.4×10^{-7}	3.9×10^{-7}
10^{-3}	DH	5.3×10^{-7}	1.2×10^{-4}		4.9×10^{-6}
	PB	1.5×10^{-6}	9.5×10^{-4}	5.6×10^{-6}	5.3×10^{-6}
10^{-4}	DH	5.3×10^{-6}	1.2×10^{-2}		6.1×10^{-5}
	PB	1.4×10^{-5}	8.0×10^{-2}	6.4×10^{-5}	6.3×10^{-5}

[a] L_p was calculated from eq 47 (DH) or obtained by interpolation in Table III of ref 10 (PB). τ_{axi} and τ_{eff} were calculated from eq 46 and 45 (with $S_2 = 0$), respectively. τ_{rad} was calculated from eq 36 and A7. Parameter values were as in Table III for NaPSS with $\alpha = 1$.

axial counterion diffusion does not significantly affect the relaxation behavior at the polyion concentrations of interest here. (The reduction of τ_{eff}, brought about by axial diffusion, is at most ca. 20%, which, if neglected, would lead to an underestimation of $\bar{\chi}_\delta$ by less than 10%.) Similar conclusions hold in the presence of added salt under the experimental conditions of Figure 6. It should be noted also that the values of τ_{axi} quoted in Table V are lower limits (for a given L_p), since correlations between the counterions, which are present at a very high concentration near the polyion, tend to reduce the effective diffusion coefficient from its infinite-dilution value given in Table III. The conclusion, then, is that we are justified in treating the polyion as a straight cylinder and to neglect the second term in eq 45. Furthermore, according to the PB theory, $L_p > L_c$ even for 0.1 mol dm^{-3} NaPSS with $N = 87$, so it is reasonable to use L_c as the characteristic length in eq 44.

Conclusions

We now recapitulate the main conclusions from this study and indicate how the theory may be generalized. Several motional degrees of freedom have been considered as candidates for the slow efg fluctuation that gives rise to ΔR_2. We have found that the extensive ΔR_2 data reported by LBL[28] can be quantitatively explained by the translational diffusion of counterions from one polyion to another. There is thus no need, for the experimental conditions that we have considered, to invoke polyion reorientation or counterion diffusion along the curved polyion axis. Furthermore, it appears that the relaxation behavior in these systems is unaffected by any changes in solution structure[28] that might accompany dilution or protonation of the polyion.

The locally averaged, residual efg experienced by a counterion, which is the only freely adjustable parameter in the theory, was found to be ca. 70 kHz. This value is consistent with results from quadrupolar line splittings in systems with similar interfacial structure. The insensitivity of the residual efg to dilution and polyion protonation indicates that it is generated mainly by local short-range interactions, rather than directly by the inhomogeneous charge distribution.

The present theory, while apparently sufficient for the data considered here, may be generalized in several respects. The two states may be replaced by a larger number of discrete states or by a continuously decaying residual efg. However, because of the local origin of efg (vide supra), this would not appreciably alter our conclusions.

The PB mean-field diffusion model, that we have adopted, implies a vanishing counterion residence time at the polyion surface. A finite residence time could, however, be introduced into the model by adding to the PB potential a short-ranged potential of mean force of suitable shape. Chemical specificity could then be parametrized via the barrier height. We emphasize that the present analysis does not rule out the possibility of a finite counterion–polyion association time, as long as it is short compared to the radial diffusion time, τ_{rad}. A more detailed insight into these matters would require an analysis of the short-time behavior of the efg correlation function, as revealed by measurements of R_1 and R_2^-.

The relaxation theory developed here may be regarded as a limiting form of a more general theory. As the long-range Coulomb interaction is attenuated by reducing the polyion charge density or by increasing the polyion or salt concentration, the Γ–Ω_{LC} time-scale separation ceases to be a valid approximation. A general treatment,[30] which avoids this time-scale separation, demonstrates that the simple result of eq 35 for $J_s(0)$ emerges in the limit of strong Coulomb coupling. Under conditions where eq 35 does not apply, the correlation function does not exhibit a pronounced long-time tail and so ΔR_2 should be small. However, a generalized version of the theory would still be needed to interpret R_1 data.

Finally, we note that certain elements of the present theory should be applicable, not only to solutions of linear polyelectrolytes, but also to solutions of other charged macromolecules and molecular aggregates. However, the very long correlation times discussed here are expected to be a unique feature of isotropic systems with at least one very large dimension.

Acknowledgment. We are grateful to Dr. M. Whittaker for performing the NMR measurements, to Dr. D. Y. C. Chan for helpful discussions, and to Dr. J. C. Leyte for comments on an early version of the paper. Part of this work was performed while enjoying the generous hospitality of the Department of Applied Mathematics at the Australian National University. This work was supported by grants from the Swedish Natural Science Research Council.

Appendix A

Analytic Results for the Cylindrical-Cell Model. In this appendix we present some analytical results for the distribution and dynamics of counterions in polyelectrolyte solutions. The results are valid under the model assumptions given above, with the further restriction that the system contains no added salt. We define two dimensionless quantities

$$C \equiv |ze\sigma|a/(2\epsilon_0\epsilon_r k_B T) \tag{A1}$$

$$\eta \equiv \ln (b/a) \tag{A2}$$

The equations take on slightly different forms depending on whether one has the low-charge case with

$$C < \eta(1 + \eta)^{-1} \tag{A3a}$$

or the high-charge case with

$$C > \eta(1 + \eta)^{-1} \tag{A3b}$$

We shall give only the high-charge results. The corresponding low-charge expressions are obtained simply by replacing s by is everywhere. This dimensionless parameter s is the solution to the transcendental equation

$$(1 + s^2)[1 + s \cot (s\eta)]^{-1} = C \tag{A4}$$

The mean electrostatic potential is given by[4-6]

$$\psi(r) = \frac{2k_B T}{ze} \ln \left\{ \frac{r}{b} \left[\cos \left(s \ln \frac{b}{r} \right) + \frac{1}{s} \sin \left(s \ln \frac{b}{r} \right) \right] \right\} \tag{A5}$$

When this result is inserted into eq 6 (with $n_s = 0$), we get after integration

$$P = 1 - \frac{1}{C} \left[1 - \frac{1 - s \tan \left(s \ln \frac{b}{a + \delta} \right)}{1 + \frac{1}{s} \tan \left(s \ln \frac{b}{a + \delta} \right)} \right] \tag{A6}$$

The mean residence time in the cell is obtained by substituting eq A5 and 10 into eq 13, using eq 5 and evaluating one integral. The result is

$$\tau_{cell}\left(\frac{D}{b^2}\right) = \left\{\frac{1}{4C} - \frac{1}{(1+s^2)} + \frac{(5+s^2)C}{4(1+s^2)^2}\right\} + \left(\frac{a}{b}\right)^2\left\{\frac{(1+s^2)}{2s^2C^2}\sin^2(s\eta) - \frac{1}{4C} - \frac{C}{4s^2}\left[1 + \frac{s(3-s^2)}{(1+s^2)^2}\sin(2s\eta) - \frac{(1-3s^2)}{(1+s^2)^2}\cos(2s\eta)\right]\right\} \quad (A7)$$

The corresponding mean residence time for a planar cell has been given previously.[65]

Appendix B

Decomposition of the Correlation Function. In this appendix we give a formal derivation of the decomposition of a temporal autocorrelation function resulting from time-scale separation of the stochastic variables. Consider the temporal autocorrelation function of some classical observable $A(t)$

$$G(t) = \langle A^*(0)\, A(t)\rangle \quad (B1)$$

Assume that the time dependence of $A(t)$ is due to a set, $\mathbf{X}$, of stochastic variables. $G(t)$ may then be expressed in terms of the joint equilibrium probability density, $f(\mathbf{X})$, and the joint transition probability density, $f(\mathbf{X};t|\mathbf{X}^0)$, as

$$G(t) = \int d\mathbf{X}^0\, f(\mathbf{X}^0)\, A^*(\mathbf{X}^0) \int d\mathbf{X}\, f(\mathbf{X};\, t|\mathbf{X}^0)\, A(\mathbf{X}) \quad (B2)$$

These probability densities satisfy the following normalization conditions:

$$\int d\mathbf{X}\, f(\mathbf{X}) = 1 \quad (B3a)$$

$$\int d\mathbf{X}\, f(\mathbf{X};t|\mathbf{X}^0) = 1 \quad (B3b)$$

$$\int d\mathbf{X}^0\, f(\mathbf{X}^0)\, f(\mathbf{X};t|\mathbf{X}^0) = f(\mathbf{X}) \quad (B3c)$$

(For stochastic variables associated with a discrete sample space, the integrals are replaced by sums.)

Assume now that the set $\mathbf{X}$ may be divided into two subsets, $\mathbf{X}_f$ and $\mathbf{X}_s$, such that all members of $\mathbf{X}_s$ remain essentially constant over periods of time sufficient for statistical averaging of all members of $\mathbf{X}_f$. In other words: asume the existence of a time, τ, such that

$$f(\mathbf{X};\tau|\mathbf{X}^0) = f(\mathbf{X}_f)\, \delta(\mathbf{X}_s - \mathbf{X}_s^0) \quad (B4)$$

The fast and slow subsets must then be statistically independent at all times, i.e.

$$f(\mathbf{X};t|\mathbf{X}^0) = f(\mathbf{X}_f;t|\mathbf{X}_f^0)\, f(\mathbf{X}_s;t|\mathbf{X}_s^0) \quad (B5)$$

Since

$$\lim_{t\to\infty} f(\mathbf{X};t|\mathbf{X}^0) = f(\mathbf{X}) \quad (B6)$$

it follows from eq B5 that

$$f(\mathbf{X}) = f(\mathbf{X}_f)\, f(\mathbf{X}_s) \quad (B7)$$

The quantity A is now divided into two parts as

$$A(\mathbf{X}) = A_f(\mathbf{X}_f,\mathbf{X}_s) + A_s(\mathbf{X}_s) \quad (B8a)$$

where

$$A_f(\mathbf{X}_f,\mathbf{X}_s) \equiv A(\mathbf{X}) - A_s(\mathbf{X}_s) \quad (B8b)$$

$$A_s(\mathbf{X}_s) \equiv \int d\mathbf{X}_f\, f(\mathbf{X}_f)\, A(\mathbf{X}) \quad (B8c)$$

We then insert eq B5, B7, and B8a into eq B2 and make use of eq B3 and B8b to obtain the desired result

$$G(t) = G_f(t) + G_s(t) \quad (B9a)$$

where

$$G_f(t) \equiv \int d\mathbf{X}_s^0\, f(\mathbf{X}_s^0) \int d\mathbf{X}_f^0\, f(\mathbf{X}_f^0)\, A_f^*(\mathbf{X}_f^0,\mathbf{X}_s^0) \times \int d\mathbf{X}_f\, f(\mathbf{X}_f;t|\mathbf{X}_f^0)\, A(\mathbf{X}_f,\mathbf{X}_s^0) \quad (B9b)$$

$$G_s(t) \equiv \int d\mathbf{X}_s^0\, f(\mathbf{X}_s^0)\, A_s^*(\mathbf{X}_s^0) \int d\mathbf{X}_s\, f(\mathbf{X}_s;t|\mathbf{X}_s^0)\, A_s(\mathbf{X}_s) \quad (B9c)$$

Note that while $G_f(t)$ depends on $f(\mathbf{X}_s^0)$, it is independent of the dynamics of the slow subset.

Appendix C

Effect of Orientational Correlation between Polyions. This appendix is devoted to a derivation of an orientational correlation function determined by the translational diffusion of counterions among orientationally correlated polyions. The reduced correlation function, defined in eq 32 of the main text, may also be written

$$\tilde{G}_s(t) = 5\int d\Omega_{LC}^0\, f(\Omega_{LC}^0) \int d\Omega_{LC}\, f(\Omega_{LC};t|\Omega_{LC}^0)\, D_{00}^2(\Omega_{LC}^0)\, D_{00}^2(\Omega_{LC}) \quad (C1)$$

We define a transition as an event whereby a counterion diffuses from the perturbed region ($r < a + \delta$) of one cell to that of a neighboring one. The transition probability density may then be written

$$f(\Omega_{LC};t|\Omega_{LC}^0) = \sum_{N=0}^{\infty} P_N(t)\, f_N(\Omega_{LC_N}|\Omega_{LC_0}) \quad (C2)$$

$P_N(t)$ is the probability that the counterion has undergone precisely N transitions at time t. (Note that all of the $N+1$ cells that have been visited at time t are not necessarily distinct.) The quantity $f_N(\Omega_{LC_N}|\Omega_{LC_0})\, d\Omega_{LC_N}$ is the probability that, after precisely N transitions, the counterion resides in a cell with orientation within $d\Omega_{LC_N}$ of Ω_{LC_N}, given that it was initially in a cell with orientation Ω_{LC_0}. Obviously, $f_0 = \delta(\Omega_{LC} - \Omega_{LC}^0)$, where $\Omega_{LC}^0 \equiv \Omega_{LC_0}$.

We assume that the transitions are uncorrelated in time, i.e., that they are Poisson distributed

$$P_N(t) = (1/N!)(t/\tau_{rad})^N \exp(-t/\tau_{rad}) \quad (C3)$$

where τ_{rad} is the mean time between transitions (cf. the discussion preceding eq 35). Combining eq C1–C3, we get

$$\tilde{G}_s(t) = \exp\left(-\frac{t}{\tau_{rad}}\right) \sum_{N=0}^{\infty} \frac{1}{N!}\left(\frac{t}{\tau_{rad}}\right)^N G_N \quad (C4)$$

where

$$G_N \equiv 5\int d\Omega_{LC_0}\, f(\Omega_{LC_0}) \int d\Omega_{LC_N}\, f_N(\Omega_{LC_N}|\Omega_{LC_0})\, D_{00}^2(\Omega_{LC_0})\, D_{00}^2(\Omega_{LC_N}) \quad (C5)$$

We now proceed to evaluate G_N. First we note that in a rotationally invariant (isotropic) fluid $f_N(\Omega_{LC_N}|\Omega_{LC_0})$ can depend only on the relative orientation $\Omega_{C_0C_N}$, i.e.

$$f_N(\Omega_{LC_N}|\Omega_{LC_0})\, d\Omega_{LC_N} = f_N(\Omega_{C_0C_N})\, d\Omega_{C_0C_N} \quad (C6)$$

From the closure relation for the D elements,[51] we have

$$D_{00}^2(\Omega_{LC_N}) = \sum_k D_{0k}^2(\Omega_{LC_0})\, D_{k0}^2(\Omega_{C_0C_N}) \quad (C7)$$

Inserting eq C6 and C7 into eq C5 and performing the Ω_{LC_0} integration, using eq 17 and the orthogonality of the D elements,[51] we get

$$G_N = \int d\Omega_{C_0C_N}\, f_N(\Omega_{C_0C_N})\, D_{00}^2(\Omega_{C_0C_N}) \quad (C8)$$

We shall describe the interpolyion structure in the polyelectrolyte solution entirely in terms of the orientational pair correlation $f_1(\Omega_{LC_2}|\Omega_{LC_1})$, or $f(\Omega_{C_1C_2})$, of neighboring (or nearby) cells. That is, we neglect triplet and higher correlations. Furthermore, we treat previously visited cells as statistically equivalent to all other cells. The sequence of transitions can then be treated as a Markov process, which obeys the Chapman–Kolmogorov equation (for $N \geq 1$)

$$f_N(\Omega_{LC_N}|\Omega_{LC_0}) = \int d\Omega_{LC_{N-1}} f_1(\Omega_{LC_N}|\Omega_{LC_{N-1}}) f_{N-1}(\Omega_{LC_{N-1}}|\Omega_{LC_0}) \quad (C9)$$

Repeated application yields

$$f_N(\Omega_{LC_N}|\Omega_{LC_0}) = \int d\Omega_{LC_{N-1}} f_1(\Omega_{LC_N}|\Omega_{LC_{N-1}}) \times \int d\Omega_{LC_{N-2}} f_1(\Omega_{LC_{N-1}}|\Omega_{L-C_{N-2}})... \times \int d\Omega_{LC_1} f_1(\Omega_{LC_2}|\Omega_{LC_1}) f_1(\Omega_{LC_1}|\Omega_{LC_0}) \quad (C10a)$$

or, using eq C6

$$d\Omega_{C_0C_N} f_N(\Omega_{C_0C_N}) = d\Omega_{C_{N-1}C_N} f(\Omega_{C_{N-1}C_N}) \int d\Omega_{C_{N-2}C_{N-1}} f(\Omega_{C_{N-2}C_{N-1}})... \int d\Omega_{C_0C_1} f(\Omega_{C_0C_1}) \quad (C10b)$$

Using the closure relation again, we have

$$D^2_{00}(\Omega_{C_0C_N}) = \sum_{k_1} D^2_{0k_1}(\Omega_{C_0C_1}) D^2_{k_10}(\Omega_{C_1N}) \quad (C11)$$

or, after repeated application

$$D^2_{00}(\Omega_{C_0C_N}) = \sum_{k_1}\sum_{k_2}... \sum_{k_{N-1}} D^2_{0k_1}(\Omega_{C_0C_1}) D^2_{k_1k_2}(\Omega_{C_1C_2}) ... D^2_{k_{N-1}0}(\Omega_{C_{N-1}C_N}) \quad (C12)$$

When eq C10b and C12 are inserted into eq C8, we get

$$G_N = \sum_{k_1}\sum_{k_2}... \sum_{k_{N-1}} \int d\Omega_{C_0C_1} f(\Omega_{C_0C_1}) D^2_{0k_1}(\Omega_{C_0C_1}) \times \int d\Omega_{C_1C_2} f(\Omega_{C_1C_2}) D^2_{k_1k_2}(\Omega_{C_1C_2})... \times \int d\Omega_{C_{N-1}C_N} f(\Omega_{C_{N-1}C_N}) D^2_{k_{N-1}0}(\Omega_{C_{N-1}C_N}) \quad (C13)$$

The orientational pair correlation can be expanded as (cf. eq 7)

$$f(\Omega_{C_{N-1}C_N}) = \sum_{l=0}^{\infty} \left(\frac{2l+1}{8\pi^2}\right) S_l D^l_{00}(\Omega_{C_{N-1}C_N}) \quad (C14)$$

where the lth-rank order parameter S_l is defined as in eq 8. Inserting eq C14 into eq C13 and performing the integrations, making use of the orthogonality of the D elements, we get

$$G_N = (S_2)^N \quad (C15)$$

Substitution into eq C4 leads to the desired result

$$\tilde{G}_s(t) = \exp[-\{(1 - S_2)/\tau_{rad}\}t] \quad (C16)$$

which, on combination with eq 30, yields eq 37.

Appendix D

Experimental Details. Sodium poly(styrenesulfonate) (M_r = 35000 and 88% monosulfonation according to the manufacturer) was obtained from Pressure Chemical Co. and used without further purification. The water was freshly purified through the following steps: mixed-bed ion-exchange resin, distillation, charcoal, and distillation.

Prior to use, all glassware was soaked for 1 day in hot 7% HNO_3 and subsequently rinsed in purified water. To avoid any interfering NMR signal[60] from sodium present in borosilicate glass, quartz sample tubes (10-mm o.d.) were used. Sample volumes were 6 cm^3, including 1 cm^3 of distilled D_2O for the locking signal.

^{23}Na absorption spectra were recorded at 51.91 MHz on a Bruker CXP 200 Fourier-transform spectrometer. An internal ^2H lock was used and the resolution was adjusted to better than 1 Hz. The $\pi/2$ pulse width was 40 μs, the dwell time 250 μs, and the acquisition time 0.15 s. The number of acquisitions was sufficient to yield a signal-to-noise ratio of 90 or better. Over the recorded spectral width (2000 Hz) the amplitude of any base-line distortion was always less than the peak-to-peak noise. The temperature was kept constant at 20 °C by the passage of thermostated air through the probe.

Recorded absorption spectra were fitted to the theoretical expression[52] for the biexponential decay of the transverse magnetization of a spin $^3/_2$ nucleus. Six parameters were fitted: the two relaxation rates (R_2^+ and R_2^-), the spectrum amplitude, the distance to the true base line, the resonance frequency, and a first-order phase correction. The latter four parameters never deviated significantly from the subjective input estimates. From each spectrum 96 data points, equidistant in frequency, were analyzed, spanning a range of 375 Hz symmetrically around the absorption maximum. Variations in the number of data points (48 or 96) or in the spectral width (94, 188, or 375 Hz) affected, in a nonsystematic way, the deduced relaxation rates by 10% or less.

Appendix E

Effect of Axial Counterion Diffusion. In this appendix we consider the joint correlation function for radial and axial counterion diffusion in a polyelectrolyte solution. Noting that $D^l_{00}(\Omega) = P_l(\cos\theta)$, the lth-degree Legendre polynomial, we may rewrite eq 32 as

$$\tilde{G}_s(t) = 5\int_{-1}^{1} d\zeta_0 f(\zeta_0) P_2(\zeta_0) \int_{-1}^{1} d\zeta f(\zeta;t|\zeta_0) P_2(\zeta) \quad (E1)$$

where $\zeta \equiv \cos\theta_{LC}$. The equilibrium distribution of polyion orientations in an isotropic system is

$$f(\zeta) = 1/2 \quad (E2)$$

For simplicity we assume that the DCA is valid and that the cells are completely uncorrelated ($S_2 = 0$). If, furthermore, the axial and radial motions are statistically independent, the transition probability density may be decomposed as

$$f(\zeta;t|\zeta_0) = f_{axi}(\zeta;t|\zeta_0) P_{cell}(t) + f(\zeta)[1 - P_{cell}(t)] \quad (E3)$$

where the probability that the spin remains in the cell at time t is

$$P_{cell}(t) = e^{-t/\tau_{cell}} \quad (E4)$$

The axial transition probability density can be expressed as

$$f_{axi}(\zeta;t|\zeta_0) = \int_0^{\infty} ds\, f(\zeta;s|\zeta_0) f(s;t) \quad (E5)$$

where s is the curvilinear displacement coordinate along the polyion axis. In the PB approximation, there is no field in the axial direction so that the appropriate propagator to use in eq E5 is that for one-dimensional free diffusion

$$f(s;t) = (\pi Dt)^{-1/2} \exp[-s^2/(4Dt)] \quad (E6)$$

The persistence length, L_p, enters via the probability, $f(\zeta;s|\zeta_0)\, d\zeta$, of having an orientation within $d\zeta$ of ζ after a contour displacement s, given that the orientation was ζ_0 at $s = 0$. We shall take

$$f(\zeta;s|\zeta_0) = 1/2 + [\delta(\zeta-\zeta_0) - 1/2]e^{-s/L_p} \quad (E7)$$

It is easy to verify that this distribution is consistent with the definition[66] of the persistence length, which may be written

$$L_p \equiv \frac{1}{\zeta_0}\int_0^{\infty} ds\, \langle\zeta\rangle = \frac{1}{\zeta_0}\int_0^{\infty} ds \int_{-1}^{1} d\zeta\, \zeta f(\zeta;s|\zeta_0) \quad (E8)$$

Combining eq E1–E7, performing the angular integrations, and making use of the orthogonality of the Legendre polynomials, we obtain

$$\tilde{G}_s(t) = (\pi Dt)^{-1/2} e^{-t/\tau_{cell}} \int_0^{\infty} ds \exp\left[-\left(\frac{s}{L_p} + \frac{s^2}{4Dt}\right)\right] \quad (E9)$$

and, after carrying out the displacement integral[67]

$$\tilde{G}_s(t) = \exp[-(1/\tau_{cell} - D/L_p^2)t]\ \mathrm{erfc}\ [(Dt)^{1/2}/L_p] \quad (E10)$$

This correlation function clearly leads to a non-Lorentzian spectral density with a complicated frequency dependence. However, if we are interested only in the zero-frequency spectral density, we can define an effective correlation time

$$\tau_{eff} \equiv \int_0^{\infty} dt\, \tilde{G}_s(t) \quad (E11)$$

Inserting $\tilde{G}_s(t)$ from eq E10 and performing the integration,[67] we get

$$1/\tau_{eff} = 1/\tau_{cell} + 1/(2\tau_{cell}\tau_{axi})^{1/2} \quad \text{(E12)}$$

where we have introduced

$$\tau_{axi} \equiv L_p^2/(2D) \quad \text{(E13)}$$

It is interesting to note that were it not for the factor $\exp(-t/\tau_{cell})$ connected with the radial diffusion, the integral in eq E11 would diverge. For translational diffusion in one or two dimensions the correlation function exhibits a long-time tail, which causes $J(0)$ to diverge. One has then left the motional narrowing regime where the conventional second-order perturbation theory of spin relaxation is valid.[25] This behavior is closely related to the well-known fact that a random lattice walker is certain to return to his starting point in one or two, but not in three, dimensions.[68]

If the relaxing interaction is modulated by several statistically independent processes, each of which would give rise to an exponentially decaying correlation function $\exp(-t/\tau_i)$, then the total correlation function is also exponential with

$$1/\tau_{eff} = \sum_i (1/\tau_i) \quad \text{(E14)}$$

In comparison with this relation, eq E12 predicts that the axial diffusion influences τ_{eff} to a lesser extent (for $\tau_{axi} \lesssim \tau_{cell}$).

Raman Spectroscopic Studies of Submillimolar Surfactant Solutions. Concentration Dependence of the C-H Stretching Raman Lines

Keij Kamogawa,* Kazuo Tajima,† Kazuo Hayakawa, and Teizo Kitagawa

Institute for Molecular Science, Myodaiji, Okazaki, Aichi, 444 Japan, and Department of Chemistry, Faculty of Science, Tokyo Metropolitan University, Setagaya, Tokyo, 158 Japan *(Received: August 17, 1983)*

C-H stretching Raman spectra of very dilute surfactant solutions and their concentration difference spectra were obtained with the aid of a highly sensitive optical multichannel analyzer detection system for decyl to tetradecyl sulfate in aqueous solution. By effective subtraction of the water background, profiles of the C-H spectra could be revealed even for a 0.5 mM solution, although so far the reported data have been limited mostly to concentrations above 100 mM. Upon dilution in the concentration region slightly higher than the critical micelle concentration (cmc), appreciable high-frequency shifts of the 2860- and 2900-cm^{-1} bands were elucidated in the difference spectra in addition to an intensity rise around 2950 cm^{-1}. The intensity rise appeared to be coupled with the upward shift of the 2860-cm^{-1} band irrespective of the length of the hydrocarbon chain. Since similar frequency shifts were also observed for dilution of CH_3OH with CD_3OD, one of the likely origins of the frequency shift is an intermolecular vibrational coupling of C-H bonds but is not simply a change of the surrounding polarity. Those features seem to be a general characteristic of surfactants upon the change from the micellar to molecular solvation.

Introduction

Micelle formation of surfactants in an aqueous solution brings about a discontinuous change in some molecular properties as well as macroscopic solution properties,[1,2] and their correlation is currently of spectroscopic interest. Since the Raman spectra in the C-H stretching region around 2840-2970 cm^{-1} are sensitive to the structure and environments of the hydrocarbon chain,[3,4] presumably due to a change of Fermi resonance conditions,[5] Raman spectra have been extensively used to prove the membrane properties.[6-9] The technique is also expected to provide some structural information on molecular aggregates of surfactants such as alkyl carbonates and alkyl sulfates with C_5-C_{12}.[10-13] So far the measurements have been carried out for relatively concentrated solutions, and an intensity rise around 2930 cm^{-1} observed upon dilution was interpreted in terms of only a local polarity change around the hydrocarbon chain.[10,12] The spectral intensity, however, was insufficient to extend the measurements to more dilute solutions, lower than 100 mM; hence, there have been only a few data on molecular solutions of the surfactants.

In this study, the C-H spectra of alkyl sulfates of C_{10}-C_4 were investigated to see effects of demicellization. The critical micelle concentrations (cmc) of these surfactants are several to thirty millimolar, and for the solutions below cmc a wing of the O-H stretching Raman line of solvent water dominates the Raman spectra above 3000 cm^{-1}. Therefore, in this study, a new technical development was worked out first. This enabled a long time accumulation of the spectra and effective subtraction of the water background. The C-H spectra thus obtained exhibited diffuse features, which are a result of heterogeneous broadening due to intermolecular disordering,[5] the presence of several rotamers,[3] and homogeneous broadening due to dynamic effects.[14] To analyze such a complicated system, qualitative characterization of the spectral changes in terms of the peak positions, peak heights, and the line widths is required in the first step. Accordingly, we have

* Address correspondence to this author at the Institute for Molecular Science, Myodaiji, Okazaki, Aichi, 444 Japan.
† Tokyo Metropolitan University.

(1) J. H. Fendler and E. J. Fendler, "Catalysis in Micellar and Micromolecular Systems", Academic Press, New York, 1975.
(2) J. K. Thomas, *Chem. Rev.*, **80**, 283 (1980).
(3) B. P. Gaber and W. L. Peticolas, *Biochim. Biophys. Acta*, **465**, 260 (1977).
(4) R. Mendelsohn, S. Sunder, and H. J. Bernstein, *Biochim. Biophys. Acta*, **419**, 563 (1976).
(5) R. G. Synder, S. L. Hsu, and S. Krimm, *Spectrochim. Acta, Part A*, **34**, 395 (1978).
(6) T. Taraschi and R. Mendelsohn, *J. Am. Chem. Soc.*, **101**, 1050 (1979).
(7) R. Mendelsohn and T. Taraschi, *Biochemistry*, **17**, 3944 (1978).
(8) S. P. Verma and D. F. H. Wallach, *Biochem. Biophys. Res. Commun.*, **74**, 473 (1977).
(9) M. R. Bunow and I. W. Levin, *Biochim. Biophys. Acta*, **464**, 202 (1977).
(10) K. Larsson and R. P. Rand, *Biochim. Biophys. Acta*, **326**, 245 (1973).
(11) K. Kalyanasundaram and J. K. Thomas, *J. Phys. Chem.*, **80**, 1462 (1976).
(12) J. B. Rosenholm, P. Stenius, and I. Danielsson, *J. Colloid Interface Sci.*, **57**, 551 (1976).
(13) H. Okabayashi and T. Kitagawa, *J. Phys. Chem.*, **82**, 1830 (1978).
(14) R. G. Snyder, J. R. Scherer, and B. P. Gaber, *Biochim. Biophys. Acta*, **601**, 47 (1980).

0022-3654/84/2088-2494$01.50/0